SCIENTIA PLENA
www.scientiaplena.org.br
VOL. 21, NUM. 12 2025
doi: 10.14808/sci.plena.2025.123401

Synthesis and characterization of polyurethane foam with functionalized graphene nanoplatelets

Síntese e caracterização de espumas de poliuretano com grafeno nanoplateletes funcionalizado

M. B. A. Mitrus[1]; L. R. Alves[2]*; G. M. Carriello[2]; G. M. Pegoraro[2]; D. R. Gomes[2]; A. J. Menezes[2]; M. L. Rezende[1]

[1]*Laboratório de Caracterização de Materiais Poliméricos, Faculdade de Tecnologia José Crespo Gonzales, 18013-280, Sorocaba-SP, Brasil*
[2]*Laboratório de Materiais, Programa de Pós-Graduação em Ciência dos Materiais, Universidade Federal de São Carlos, 18052-780, Sorocaba-SP, Brasil*

**lucasrepecka@estudante.ufscar.br*
(Recebido em 07 de abril de 2025; aceito em 10 de setembro de 2025)

This work presents the synthesis and characterization of polyurethane (PU) foams incorporating functionalized graphene nanoplatelets (FGN). A 2^2 factorial design was used, varying the mass ratio between isocyanate and polyol (1:1 and 1:2) and the volume of the FGN suspension (1 and 2 mL) to evaluate the influence of these variables on the final properties of the foams. The samples were characterized by Fourier-transform infrared spectroscopy (FTIR), scanning electron microscopy (SEM), X-ray diffraction (XRD), soluble fraction testing, and oil absorption capacity. FTIR results confirmed the formation of the PU structure, regardless of the presence of FGN. SEM images revealed morphological changes in the foams containing FGN, showing fractures and irregular structures attributed to interactions between the nanomaterial and the polymer matrix. Soluble fraction tests indicated variations in the degree of crosslinking of the foams, while the oil absorption assays demonstrated that the incorporation of FGN did not significantly enhance the oil absorption capacity, indicating that the presence of the nanomaterial did not substantially affect this parameter. Nevertheless, this study contributes to understanding the effects of functionalized graphene on the structure and performance of PU foams, providing insights for the development of materials with tunable properties for specific applications.
Keywords: functionalized graphene nanoplatelets, composites, polyurethanes.

Este trabalho apresenta a síntese e caracterização de espumas de poliuretano (PU) com a incorporação de nanoplaquetas de grafeno funcionalizadas (NGF). Utilizando um delineamento fatorial 2^2, variaram-se a razão mássica entre isocianato e poliol (1:1 e 1:2) e o volume da suspensão de NGF (1 e 2 mL) para avaliar a influência dessas variáveis nas propriedades finais das espumas. As amostras foram caracterizadas por espectroscopia no infravermelho por transformada de Fourier (FTIR), microscopia eletrônica de varredura (MEV), difração de raios-X (DRX), teste de fração solúvel e capacidade de absorção de óleo. Os resultados de FTIR confirmaram a formação da estrutura de PU, independentemente da presença de NGF. As imagens de MEV revelaram alterações morfológicas nas espumas com NFG, apresentando fraturas e estruturas irregulares atribuídas à interação entre o nanomaterial e a matriz polimérica. Os testes de fração solúvel indicaram variações no grau de reticulação das espumas, enquanto os ensaios de absorção demonstraram que a incorporação de NGF não promoveu um aumento significativo na capacidade de absorção de óleo, indicando que a presença do nanomaterial não interferiu de forma expressiva nesse parâmetro. Ainda assim, o estudo contribui para a compreensão dos efeitos do grafeno funcionalizado na estrutura e no desempenho de espumas de PU, fornecendo subsídios para o desenvolvimento de materiais com propriedades ajustáveis para aplicações específicas.
Palavras-chave: grafeno nanoplateletes funcionalizado, compósitos, poliuretanos.

1. INTRODUCTION

Polyurethanes (PUs) are highly versatile polymeric materials obtained through an exothermic reaction between chemical groups (-NCO) derived from isocyanates and groups (-OH) originating from polyols, which are responsible for the formation of the polymer [1, 2]. The high versatility can be explained by the diversity of chemical structures of the polyols and isocyanates that can be used in its synthesis, which are responsible for its final properties [3]. As a result, these materials can be found in the form of paints, adhesives, sealants, elastomers, thermoplastics, and

foams [4]. However, the largest use of this polymer is in the form of foams, which represent 65% of the PU market, making it the sixth most commercially traded polymer worldwide [3, 5].

Foams can be categorized as flexible, rigid, and semi-rigid, depending on their density and physical characteristics. For example, flexible foams have an open-cell structure, while rigid foams have a closed-cell structure [3]. This versatility allows these materials to be used in various industry sectors, such as furniture manufacturing, automotive, packaging, biomedical applications, construction, textiles, and many others, due to their lightness combined with excellent properties, such as mechanical strength, hardness, thermal insulation, sound absorption, and noise reduction [5-8].

Graphene is a widely researched type of material formed by a single layer of hexagonally bonded carbon atoms, known to present good mechanical, electrical and thermal properties [9]. However, its production has not yet been optimized for quickness and low cost [10]. Meanwhile, graphene nanoplatelets, which are composed of graphite, mono- and multi-layered graphene, are already produced and sold in larger scale by industry and is generally preferred when applied in combination with other nanomaterials or polymers to form composites, since it retains good properties from graphene and can be obtained at a lower cost [9, 11].

Functionalized graphene nanoplatelets (FGNs) have been combined with PU before, especially aiming to improve the mechanical and thermal properties of the polymer [12, 13]. For oil absorption, however, graphene oxide tends to be used in combination with PU, unlike FGNs, which have only been researched as oil absorbers in pristine form [14-16]. In this work, FGNs were combined with PU in different proportions through a 2^2 factorial design, characterized and evaluated for oil absorption.

2. MATERIALS AND METHODS

The materials used for the synthesis of foams with FGN were: functionalized graphene nanoplatelets with oxygen groups [17] in 0.5% vegetable oil suspension (DGD GRAPHTEK produced by DEGRAD), 2,4-diphenylmethane diisocyanate (MDI) from Redelease, and a polyol blend from Redelease.

2.1 Methodology

The adopted experimental procedure can be seen in Table 1, which was adapted from Alves et al. (2023) [18], and consists of a synthesis process called one-shot. For the preparation of the samples, approximately 2 g of polyol was weighed, and the desired amount of FGN was added using a micropipette. The polyol and FGN were stirred, and then 2 g of isocyanate was weighed in the same container. Finally, the mixture was stirred vigorously until foam formation and expansion, indicating the start of the reaction.

Table 1. Experimental procedure for the synthesis of foams with FGN.

	MR1/G1	MR1/G2	MR1:2/G1	MR1:2/G2
Mass ratio (NCO/OH)	1:1	1:1	1:2	1:2
Amount of FGN solution (mL)	1	2	1	2

The sample nomenclature used was as follows: MR refers to the mass ratio between isocyanate (-NCO) and polyol groups (-OH), in grams, while G refers to the amount of FGN, in milliliters. In this way, foams with distinct characteristics were obtained, along with control foams at 1:1 and 1:2 ratios of isocyanate to polyol. A 2^2 factorial design was carried out, resulting in 4 experiments to analyze the influence of the two variables, in this case, the amount of FGN and the isocyanate-to-polyol ratio, on the final properties of the foam, such as its chemical composition, morphology, number of cross-links, and oil absorption capacity. Additionally, for comparison purposes, two control foams with mass ratios of 1:1 and 1:2 were prepared.

2.2 Characterization and tests

All data obtained in this study were processed and plotted using Origin software, whereas the data regarding the mean pore size were obtained through the NeuraCell website.

2.2.1 Fourier-transform infrared spectroscopy (FTIR)

The materials were characterized by Fourier-transform infrared spectroscopy (FTIR) with attenuated total reflectance on a spectrophotometer (Perkin Elmer Spectrum 65). The wavelength range measured was from 4.000 to 500 cm^{-1}, with a resolution of 4 cm^{-1} and 16 scans.

2.2.2 Scanning electron microscopy (SEM)

The samples were characterized by scanning electron microscopy (SEM), using a Hitachi TM3000 microscope operating at an accelerating voltage of 5 kV without sputtering.

2.2.3 X-ray diffraction (XRD)

X-ray diffractograms were obtained using a Shimadzu X-ray diffractometer (XRD-6100). Measurement conditions used were continuous scans at a voltage of 40.0 kV, current of 30.0 mA and scan range from 5 to 35 degrees, at 2 degrees per minute.

2.2.4 Sol fraction

The soluble fraction test demonstrates the degree of crosslinking in the samples. Thus, the behavior of FGN on this property in the foams was investigated. For this, approximately 0.02 g of dry sample was weighed and immersed in xylene for 72 hours at room temperature. Subsequently, the samples were removed and dried in an oven for 24 hours at 60 °C. The soluble fraction was determined using Equation 1, where m^1 is the initial mass of the sample and m^2 is the mass after extraction in the solvent. The test was conducted in triplicate for each sample according to the following study [4].

$$SF = \frac{m_1 - m_2}{m_1} \times 100\% \quad (1)$$

2.2.5 Oil absorption test

To evaluate the oil absorption capacity of the foams, vegetable soybean oil was used. A specific amount of foam samples was cut into cubes of known mass and immersed in a beaker containing 50 mL of vegetable oil for 5 minutes at room temperature. After this period, the saturated foams were removed, and their final masses were recorded. The absorption capacity was calculated using Equation 2, where m^1 represents the initial mass of the sample before immersion, and m^2 corresponds to the mass after the absorption test. All tests were performed in triplicate for each sample, as described in Liu et al. (2013) [19].

$$A = \frac{m_2 - m_1}{m_1} \times 100\% \quad (2)$$

3. RESULTS AND DISCUSSION

3.1 Fourier-transform infrared spectroscopy (FTIR)

When observing Figure 1, both the foams containing FGN and the control samples show the hydroxyl stretching band around 3350 cm^{-1}, attributed to polyols that did not form urethane

groups [4]. In the regions of 2927 cm^{-1} and 2854 cm^{-1}, the presence of asymmetric and symmetric methyl groups is noted [20]. At 2270 cm^{-1}, residual isocyanate groups that did not participate in the reaction are identified, especially in the samples with a mass ratio of 1 [18]. Next, around 1729 cm^{-1}, the carbonyl group stretching is observed. At 1602 cm^{-1}, the presence of the C=C bond from the aromatic ring of the isocyanate is verified, along with the presence of C-N groups at 1517 cm^{-1}, confirming the successful synthesis of PU foams [21]. Finally, the band at 1227 cm^{-1}, corresponding to C-O-C groups, is observed [20]. Thus, it is concluded that the addition of FGN did not cause significant changes in any of the bands of the analyzed PU samples.

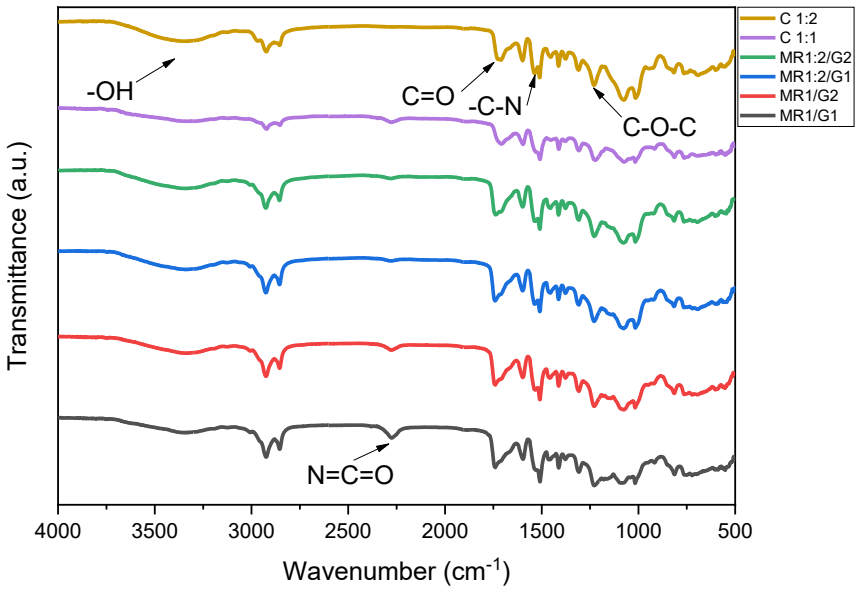

Figure 1: FTIR spectra of polyurethane foams with FGN.

3.2 Scanning electron microscopy (SEM)

Figure 2 shows the SEM images of all synthesized PU-FGN samples, along with two control samples as references, C1:1 and C1:2.

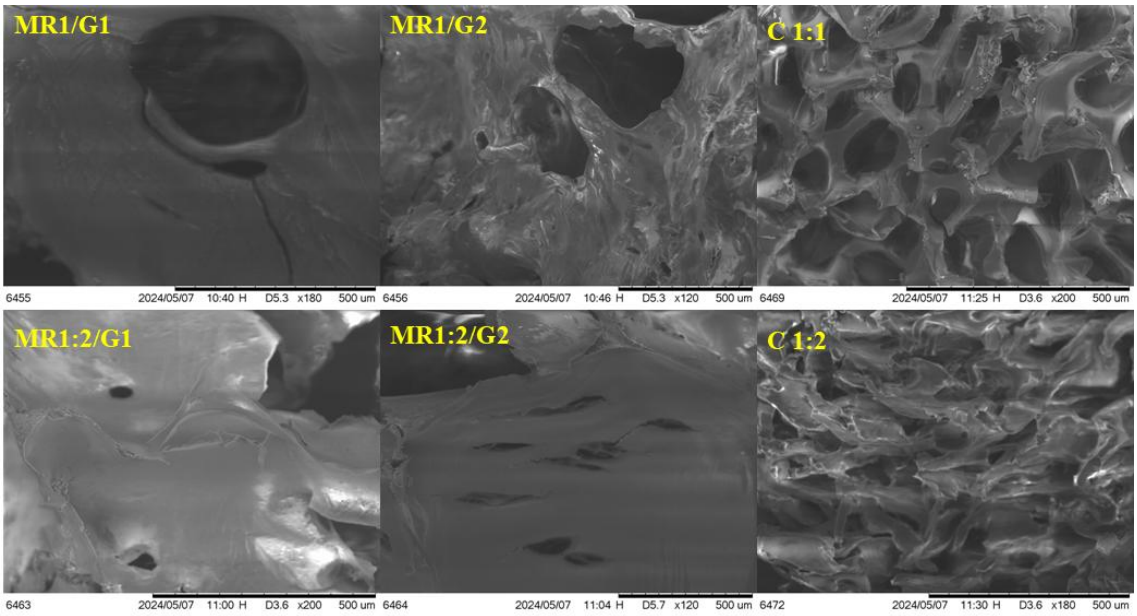

Figure 2: SEM images of the cross-section of the foams containing FGN.

When comparing the images, there is a noticeable difference in morphology, with visible tears and irregular structure in the PU-FGN foams after the addition of the functionalized graphene nanoplatelet suspension. The presence of this fractured surface in the composites is similar to that observed in previous works, to which authors attributed the covalent interaction between the FGN and the polymeric chains [12]. However, if the filler proportion is too high, or if non-functionalized graphene nanoplatelets are used, this may lead to more aggregation [12, 13].

Table 2 shows the mean pore size in two and three dimensions, as well as the standard deviation of the pores in 3D.

Table 2. Mean cell size in two and three dimensions, with the corresponding standard deviations of the cell size in 3D.

Sample	Mean cell size 2D (μm)	Mean cell size 3D (μm)	Standard deviation cell size 3D (μm)
C 1:1	128,947	164,149	50,708
C 1:2	106,36	135,405	32,814
MR1/G1	384,535	489,513	0
MR1/G2	245,418	312,417	172,419
MR1:2/G1	199,215	253,601	115,286
MR1:2/G2	230,823	293,838	28,692

It was observed that in the control samples (without FGN), the excess polyol (1:2) resulted in smaller pores, with mean diameters ranging from approximately 135 to 164 μm, whereas the 1:1 ratio presented slightly larger pores. In contrast, in the foams with a 1:1 ratio and FGN addition (1 to 2 mL), the pores were about three times larger than those of the corresponding control foam. For the foams with excess polyol, the incorporation of FGN also increased the mean pore size compared to the 1:2 control, with this effect being more pronounced as the FGN content increased. This result differs from several reports in the literature, where the addition of graphene generally leads to a reduction in pore size in PU foams [22-24]. Furthermore, the foams became more irregular, presenting pores with less uniform shapes. This behavior may be related to the dispersion of FGN in vegetable oil suspension, which could promote morphological defects and affect cell formation during foaming.

No aggregation was observed in any of the samples, which may have been a result of using a low proportion of FGNs, since only a maximum of 2 mL of the 0.5% FGN suspension was added during synthesis. In comparison, previous works that combined polyurethane and graphene nanoplatelets only reached noticeable agglomeration when the filler was present in a proportion of around 1.5 to 2.0 wt% [12, 25].

3.3 X-ray diffraction (XRD)

Figure 3 shows the diffractograms of the foams prepared with mass ratios of 1:1 and 1:2, with graphene contents of 1 and 2 mL, as well as the control foams prepared under the same conditions without graphene, for comparison purposes.

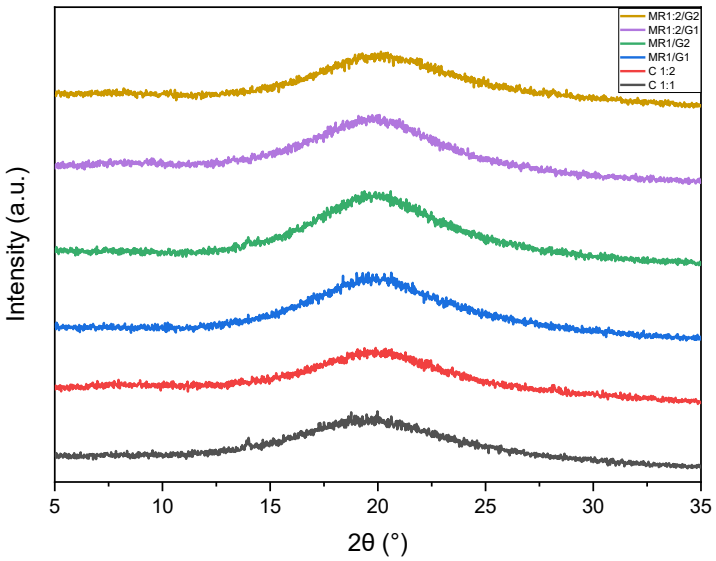

Figure 3: Diffraction patterns of the foams containing FGN.

Figure 3, which contains the diffractogram of the samples, shows evidence of a broad band around 19°, characteristic of polyurethanes with low crystallinity. The absence of peaks near 11° is also noted [26], which reinforces that the analyzed polyurethane is of the soft segment type [18].

3.4 Soluble fraction

Figure 4 shows the data on the soluble fraction of conventional foams and foams containing FGN. The sample with an MR of 1:1 and 2 mL of FGN exhibited the highest soluble fraction. This behavior can be attributed to the possible presence of residual oligomers in the sample, which result in a decrease in crosslinking [27], as well as to changes in the cellular structure of the foams, which became less porous, as observed in the SEM image in Figure 2.

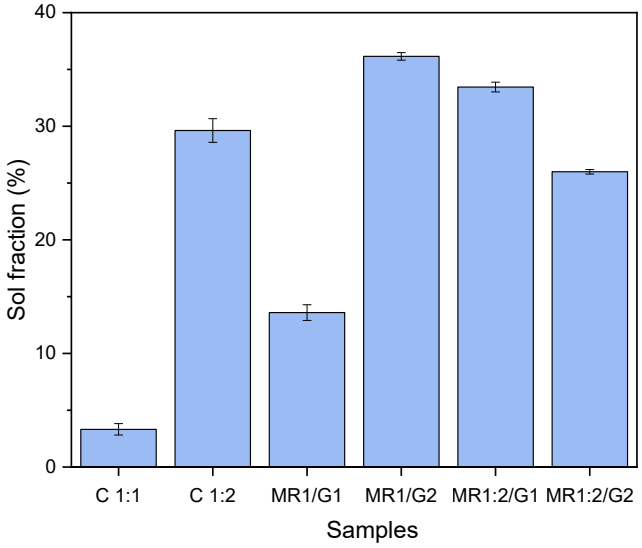

Figure 4: Sol fraction values for the foams containing FGN.

In the case of the MR1/G1 sample, a reduction was observed in the soluble fraction and an increase in crosslinking compared to MR1/G2. This indicates that FGN affects the crosslinking

of the foams, making them less crosslinked. Thus, the higher the soluble fraction, the lower the foam crosslinking will be and, consequently, the more flexible its structure, which may result in the formation of larger pores, as observed in Table 2 [4, 28]. It is worth noting that FGN is dispersed in vegetable oil.

The results obtained for the soluble fraction are in agreement with the data presented in Figure 1 (FTIR), where high soluble fractions indicate a lower extent of molecular crosslinking. Consequently, there is a reduction in the degree of crosslinking of the material structure, giving it characteristics of greater flexibility [4]. This can be observed between the bands of 3000 cm^{-1} and 3500 cm^{-1}, related to the OH group.

3.5 Oil absorption

Observing Figure 5, it is noted that the samples C 1:1, MR1/G1, and MR1/G2, within the margin of error, were similar to each other, just as the samples C 1:2, MR1:2/G1, and MR1:2/G2 were also similar to one another (C being the control sample). Comparing this with Table 1, it is evident that the samples that showed higher oil absorption were those with a greater amount of polyol. The control samples reveal that the C 1:2 formulation exhibited the highest absorption capacity (~850%), suggesting that the excess polyol favors the formation of a more porous structure, which, in turn, facilitates oil retention [29, 30]. This observation is in line with reports in the literature showing that increasing the isocyanate content generally leads to larger cell sizes; however, in the present study, the excess of polyol had the opposite effect, resulting in smaller cell sizes, as demonstrated in Table 2 [31]. In contrast, the MR1/G1 and MR1/G2 formulations, with a 1:1 ratio, showed low absorption capacities (~300%), even with the increased concentration of FGN, indicating that the mere incorporation of the nanomaterial is not sufficient to promote significant improvements in this property.

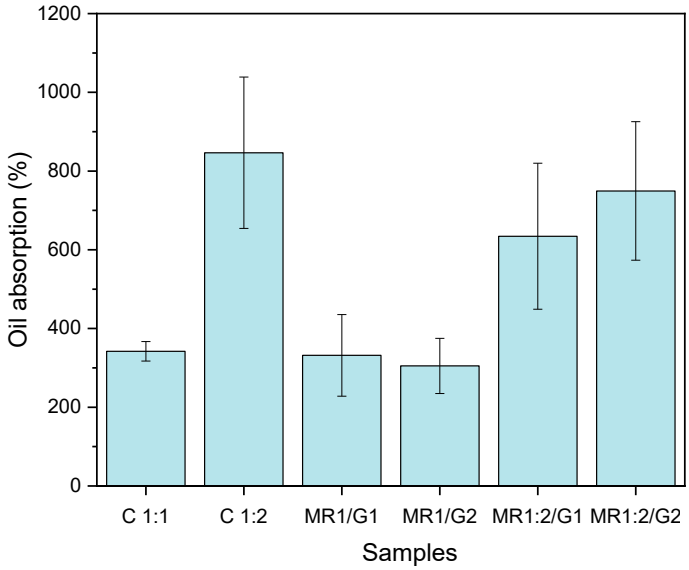

Figure 5: Vegetable oil absorption values for the foams containing FGN.

4. CONCLUSION

The synthesis and characterization of PU foams incorporating FGNs demonstrated that the addition of FGNs does not significantly alter the chemical structure of the foams, as confirmed by FTIR analysis. However, morphological changes observed through SEM images suggest an interaction between the FGNs and the PU matrix, resulting in a more fractured and irregular surface structure. The sol fraction analysis indicated that the presence of FGNs may influence the degree of crosslinking in the polymer network. Furthermore, oil absorption tests showed that the

addition of FGNs did not lead to a significant improvement in oil uptake. In contrast, increasing the polyol content relative to isocyanate in the formulation resulted in higher oil absorption capacities. Overall, the incorporation of FGNs into PU foams through a simple one-shot process proved to be an effective strategy to tailor the morphology of the material. Although no significant improvement in oil absorption was observed with FGNs, the approach opens new perspectives for controlling structural properties and exploring advanced functional applications.

5. ACKNOWLEGDMENTS

This study was financed in part by the Coordenação de Aperfeiçoamento de Pessoal de Nível Superior – Brasil (CAPES) – Finance Code 001.

6. REFERENCES

1. Alves LR, Carriello GM, Pegoraro GM, et al. Aplicações de enzimas em poliuretano: uma revisão das dissertações e teses brasileiras. Disciplinarum Scientia | Naturais e Tecnológicas. 2022;23(2):99-112. doi: 10.37779/nt.v23i2.4313
2. Alves LR, Carriello GM, Pegoraro GM, et al. A utilização de óleos vegetais como fonte de polióis para a síntese de poliuretano: uma revisão. Disciplinarum Scientia | Naturais e Tecnológicas. 2021;22(1):99-118. doi: 10.37779/nt.v22i1.3711
3. Peyrton J, Avérous L. Structure-properties relationships of cellular materials from biobased polyurethane foams. Mater Sci Eng: R: Reports. 2021;145:100608. doi: 10.1016/j.mser.2021.100608
4. Repecka Alves L, Miraveti Carriello G, Manassés Pegoraro G, et al. Green polyurethane foams: Replacing petrochemical polyol with castor oil through factorial design. J Polym Res. 2024;31(8):227. doi: 10.1007/s10965-024-04077-2
5. Zhao X, Liu Y, Lv Y, et al. Research on lignin-modified flexible polyurethane foam and its application in sound absorption. J Indd Eng Chem. 2024;137:327-37. doi: 10.1016/j.jiec.2024.03.019
6. Fu Z-C, Bu F-Y, Li Z-P, et al. Enhancing flame retardancy, mechanical durability, and anti-aging property of polyurethane foam via novel cyclic phosphonate. Chem Eng J. 2024;479:147935. doi: 10.1016/j.cej.2023.147935
7. Akindoyo JO, Beg MDH, Ghazali S, et al. Polyurethane types, synthesis and applications – a review. RSC Adv. 2016;6(115):114453-82. doi: 10.1039/C6RA14525F
8. Fu Y, Qiu C, Ni L, et al. Cell structure control and performance of rigid polyurethane foam with lightweight, good mechanical, thermal insulation and sound insulation. Constr Build Mater. 2024;447:138068. doi: 10.1016/j.conbuildmat.2024.138068
9. Yee K, Ghayesh MH. A review on the mechanics of graphene nanoplatelets reinforced structures. Int Jf Eng Sci. 2023;186:103831. doi: 10.1016/j.ijengsci.2023.103831
10. Wu Y, Li Y, Zhang X. The future of graphene: preparation from biomass waste and sports applications. Molecules. 2024;29(8):1825. doi: 10.3390/molecules29081825
11. Sevim O, Jiang Z, Ozbulut OE. Effects of graphene nanoplatelets type on self-sensing properties of cement mortar composites. Constr Build Mater. 2022;359:129488. doi: 10.1016/j.conbuildmat.2022.129488
12. Yadav SK, Cho JW. Functionalized graphene nanoplatelets for enhanced mechanical and thermal properties of polyurethane nanocomposites. Appl Surf Sci. 2013;266:360-7. doi: 10.1016/j.apsusc.2012.12.028
13. Strankowski M, Korzeniewski P, Strankowska J, et al. Morphology, mechanical and thermal properties of thermoplastic polyurethane containing reduced graphene oxide and graphene nanoplatelets. Materials. 2018;11(1):82. doi: 10.3390/ma11010082
14. Khalilifard M, Javadian S. Magnetic superhydrophobic polyurethane sponge loaded with Fe3O4@oleic acid@graphene oxide as high performance adsorbent oil from water. Chem Enginer J. 2021;408:127369. doi: 10.1016/j.cej.2020.127369
15. Chen X, Zhang J, Chen X, et al. Reduced graphene oxide-doped porous thermoplastic polyurethane sponges for highly efficient oil/water separation. ACS Omega. 2023;8(11):10487-92. doi: 10.1021/acsomega.3c00121
16. La DD, Nguyen TA, Nguyen TT, et al. Absorption behavior of graphene nanoplates toward oils and organic solvents in contaminated water. Sustainability. 2019;11(24):7228. doi: 10.3390/su11247228

17. Alves LR, Gomes DR, de Jesus Barros MF, et al. Effect of the addition of functionalized graphene nanoplatelets to cellulose nanofibrils. Cellulose. 2025;32(10):6023-34. doi: 10.1007/s10570-025-06604-w
18. Alves LR, Carriello GM, Pegoraro GM, et al. Synthesis and characterization of polyurethane and samarium(III) oxide and holmium(III) oxide compositess. Polímeros. 2023;33:e20230039. doi: 10.1590/0104-1428.20230023
19. Liu Y, Ma J, Wu T, et al. Cost-effective reduced graphene oxide-coated polyurethane sponge as a highly efficient and reusable oil-absorbent. ACS Appl Mater Interfaces. 2013;5(20):10018-26. doi: 10.1021/am4024252
20. Gomes DR, Alves LR, Carriello GM, et al. Addition of calcium carbonate in the synthesis of flexible polyurethane foams. Scientia Plena 2024;20(4):043401. doi: 10.14808/sci.plena.2024.043401
21. Carriello GM, Alves LR, Pegoraro GM, et al. Investigation of hafnium(iv) incorporation in polyurethanes: Structural and mechanical properties. Mat Res. 2024;27:e20240132. doi: 10.1590/1980-5373-MR-2024-0132
22. Shin S-R, Lee D-S. Nanocomposites of rigid polyurethane foam and graphene nanoplates obtained by exfoliation of natural graphite in polymeric 4,4′-diphenylmethane diisocyanate. Nanomaterials. (Basel) 2022;12(4):685. doi: 10.3390/nano12040685
23. Pinto SC, Marques PAAP, Vicente R, et al. Hybrid structures made of polyurethane/graphene nanocomposite foams embedded within aluminum open-cell foam. Metals. 2020;10(6):768. doi: 10.3390/met10060768
24. Kim JM, Kim DH, Kim J, et al. Effect of graphene on the sound damping properties of flexible polyurethane foams. Macromol Res. 2017;25(2):190-6. doi: 10.1007/s13233-017-5017-9
25. Nguyen Hoang T, Jaafar M, Ahmad Zubir S. Reinforcing effect of functionalized graphene nanoplatelets in palm kernel polyol based polyurethane composite. J Reinf Plast Compos. 2024;43(5-6):301-17. doi: 10.1177/07316844231162298
26. Trovati G, Sanches EA, Claro Neto S, et al. Characterization of polyurethane resins by FTIR, TGA, and XRD. J Appl Polym Sci. 2010;115(1):263-268. doi: 10.1002/app.31096
27. Sharma C, Kumar S, Unni AR, et al. Foam stability and polymer phase morphology of flexible polyurethane foams synthesized from castor oil. J Appl Polym Sci. 2014;131(17):1-8. doi: 10.1002/app.40668.
28. Kosmela P, Hejna A, Suchorzewski J, et al. Study on the structure-property dependences of rigid pur-pir foams obtained from marine biomass-based biopolyol. Materials. 2020;13(5):1257. doi: 10.3390/ma13051257
29. Ivdre A, Abolins A, Sevastyanova I, et al. Rigid polyurethane foams with various isocyanate indices based on polyols from rapeseed oil and waste PET. Polymers. 2020;12(4):738. doi: 10.3390/polym12040738
30. Alves F, Santos V, Monticeli F, et al. Efficiency of castor oil–based polyurethane foams for oil sorption S10 and S500: Influence of porous size and statistical analysis. Polym Polymer Compos. 2021;29:096739112110403. doi: 10.1177/09673911211040360
31. Kwon O-J, Yang S-R, Kim D-H, et al. Characterization of polyurethane foam prepared by using starch as polyol. J Appl Polym Sci. 2007;103(3):1544-53. doi: 10.1002/app.25363